Article:
Olanrewaju, FO, Andrews, GE orcid.org/0000-0002-8398-1363, Li, H orcid.org/0000-0002-2670-874X et al. (3 more authors) (2023) Investigation of the heat release rate and particle generation during fixed bed gasification of sweet sorghum stalk. Fuel, 332 (Part 1). 126013. ISSN 0016-2361

https://doi.org/10.1016/j.fuel.2022.126013

Investigation of the heat release rate and particle generation during fixed bed gasification of sweet sorghum stalk

Francis O. Olanrewaju[a,b*], Gordon E. Andrews[a], Hu Li[a], Herodotos N. Phylaktou[a], Bintu G. Mustafa[c], Miss H. Mat Kiah[d]

[a]School of Chemical and Process Engineering, Faculty of Engineering and Physical Sciences, University of Leeds, LS2 9JT, United Kingdom
[b]Department of Engineering Infrastructure, National Agency for Science and Engineering Infrastructure (NASENI), Abuja, Nigeria
[c]Chemical Engineering, University of Maiduguri, Bama Road, P.M.B 1069, Maiduguri, Nigeria
[d]School of Chemical and Energy Engineering, Faculty of Engineering, Universiti Teknologi Malaysia (UTM), 81310 Skudai, Johor, Malaysia

Abstract

Sweet sorghum (SS) is an agricultural crop that is produced commercially in Nigeria. The crop has a high biowaste energy in its stalk, which is an attractive source of bioenergy in rural areas where it is produced. The residue–to-produce ratio (RPR) of the crop is 1.25 kg of biowaste for 1 kg of SS produced. The solid residue that results from the crop can be subjected to gasification to produce combustible gases: carbon monoxide (CO), hydrocarbon gases (total hydrocarbons) and hydrogen. The combustible gases can be piped into a burner for heat or into a Compression Ignition (CI) engine for electricity generation. This will enhance energy security as well as energy equity in rural areas in Nigeria and sub-saharan African countries where the crop is also produced. This research was aimed at optimising the gasification of SS stalk residue to maximise the yield of combustible gases from the first stage of the process. The restricted ventilation cone calorimeter method was used to gasify SS stalks on a laboratory scale. The test was carried out at air flow rates per exposed flat surface area of 9, 11.2, 12.9, 14.3, 15.5, 16.3, and 19.2 g/s.m^2 respectively, which controls the gasification rate or power output. The speciation of the gases that evolved from the gasification of the biomass

* Corresponding author. Tel.: +447503114068; +2347030285759
E-mail addresses: sonictreasure@gmail.com (F.O. Olanrewaju), h.li3@leeds.ac.uk (H. Li), g.e.andrews@leeds.ac.uk (G.E. Andrews), h.n.phylaktou@leeds.ac.uk (H.N. Phylaktou), bintgrem@yahoo.co.uk (B.G. Mustafa), pmmhmk@leeds.ac.uk (M.H.M. Kiah)

samples was carried out by an FTIR that was calibrated for 60 species. Current uses of biomass residues in open fire heating generates toxic fine particulate emissions and this work aimed to show that this was not a greater problem with gasification. A dynamic electrical mobility particle spectrometer (DMS500) was used to measure the particulate size distribution and concentration, as an efficient gasifier should not be generating major yields of soot, which would be a problem for a downstream reciprocating engine. The optimum equivalence ratio (Φ) for the best energy transfer to the gaseous products was 2.1, which was similar to previous work on pine using this equipment where the optimum equivalence ratio was 2.8. The hot gases efficiency at the optimum Φ was 81%, which compares well to that of 78% for pine.

Key words: biomass, gasification, equivalence ratio, particulate number

Nomenclature

AFR	Air Fuel Ratio
BGG	Biomass Gasification Gas
cc	Cubic centimeter
CGFT	Char Gasification Flue Temperature, ^{o}C
CI	Compression Ignition
Cv	Calorific Value, MJ/kg
EI	Emission Index, g/kg
FBN	Fuel Bound Nitrogen
FC	Fixed Carbon, %
GCV	Gross Calorific Value, MJ/kg
HGE	Hot Gases Efficiency, %
HHV	Higher Heating Value, MJ/kg
HRR	Heat Release Rate, kW/m^2

MFT	Maximum Flue Temperature, ^{o}C
MLR	Mass Loss Rate, g/s
PHRR	Primary Heat Release Rate, kW/m^2
PM	Particulate Matter
PN	Particle Number
RCCI	Reactivity Controlled Compression Ignition
RPR	Residue-to-Produce Ratio
SHRR	Secondary Heat Release Rate, kW/m^2
SS	Sweet sorghum
SSS	Sweet sorghum stalk
THC	Total Hydrocarbons
TGA	Thermogravimetric Analyser
THRR_mlr	Total Heat Release Rate (based on the mass loss rate), kW/m^2
THR	Total Heat Release, MJ/m^2
VM	Volatile Matter, %

1. Introduction

Sweet sorghum (SS) is a multipurpose agricultural/energy crop that is produced commercially in Nigeria. It is a multipurpose crop because the grain is used for food while the leaves are used as animal feed. Currently, in Nigeria, the usual practice is to burn most of the agricultural crop residues in the open fields preparatory to the next planting season. This practice leads to enormous wastage of energy and environmental pollution. Furthermore, electricity is not

readily available in Nigeria in the rural areas, where agricultural crops and crop residues are produced.

The stalk residue of SS is a potential source for biogas (syngas). The residue-to-produce ratio (RPR) of the crop is 1.25 [1]. The RPR of the crop is quite high. Therefore, the stalk residue of sweet sorghum is a potential feedstock for syngas. Biomass gasification produces a flammable gas from a solid biomass, such as sweet sorghum stalk (SSS) and the gas can be used for heat or fed to a micro-gas turbine [2] or a diesel electric generator for power generation. Biomass gasifier efficiencies, as energy in the hot BGG as a proportion of the energy in the biomass used, range from 62-78% [2]. There is a potential to gasify agricultural crop residues like SSS and use the resulting syngas for electricity generation in diesel generators. The aim of this work, therefore, was to optimise the gasification conditions for the production of bio-gasification gas (BGG) from SSS. Gasification is rich burning of the fuel, where the products of biomass gasification are CO and hydrogen, with hydrocarbons present as a gasification inefficiency. Optimisation of the gasifier involves determining the equivalence ratio that has the highest energy content of the product gases, as well as optimising the operating temperature for maximum energy transfer.

Much of the literature on gasifiers [3-7] is about optimising the production of hydrogen, which is not the same as optimising the energy conversion efficiency. Steam injection into gasifiers is used to increase the hydrogen production, but this does not increase the energy content. Gasifiers designed to produce hydrogen see hydrocarbons as a problem, often referred to as tars, which are removed from the gas along with their energy content. In this work the aim is to keep the gasifier outlet gases hot in the transfer to a burner or engine, so that the energy in hydrocarbons are released and this is key to the high overall energy efficiency demonstrated in this work. The gasification gas would be used to fuel a diesel electricity generation set, so that rural areas of Nigeria could have low-cost electricity fuelled by the farm agricultural residues.

Investigations have also been carried out to study the effect of syngas substitution of fossil diesel on the performance of diesel-syngas dual-fuel Reactivity Controlled Compression Ignition (RCCI) engines [8-12]. Rith et al. [8] and Kousheshi et al. [9] utilised real syngas in their investigations while Mahgoub et al. [10], Guo et al. [11] and Olanrewaju et al. [12] utilised simulated syngas in their investigations. These works confirm the feasibility of the use of diesel-syngas dual fuel in RCCI engines for power generation. An RCCI engine works by using the BGG injected into the engine turbocharger inlet, with start of combustion timing controlled by a diesel or biodiesel pilot injection near TDC.

Irshad [13] used the Cone Calorimeter method, used in the present work, with pine wood to determine the gasifier optimum equivalence ratio, Ø and thermal efficiency of 2.8 and 78% respectively. Irshad [14] developed the methodology for using the Cone Calorimeter as a gasifier using the restricted ventilation enclosure around the solid fuel combustion section of the equipment. By varying the air supply to the enclosure, the gasification equivalence ratio could be varied. The methodology of Irshad [13] was used in the present work. The optimum equivalence ratio and Hot Gases Efficiency (HGE) for the gasification of sweet sorghum stalk residue were compared to those of other waste agricultural biomasses (grain sorghum stalk, corn stalk, and pine wood).

Gasification involves very rich combustion and a possible problem is that gasification can form soot, as equilibrium predictions show soot as a gasification product for Ø>~3 [15]. Also, fine particulate emissions from biomass fire burning (lean combustion) for cooking in African villages is a health problem due to inhalation of ultra-fine particles. It would be desirable to show that the gasification of biomass to produce a clean gas fuel solved this health problem in the use of biomass for direct open fire heat. Emissions of ultra fine particles from the gasifier would be undesirable, so the Particle Number (PN), Particulate Matter (PM) emissions and size where the maximum PN occurred were investigated.

The particle emissions in ventilation-controlled (rich burning) compartment fires for pine wood cribs [14] were found to be about 100 mg/m^3. Johansson et al. [16] reported PM emissions of

62 to 180 mg/m^3 for pellet burners (lean burning), similar to the value found for pine cribs in rich burning compartment fires [14]. Mustafa et al. [15] used the restricted ventilation cone calorimeter method to investigate the PN emissions for construction pine wood at 19.2 g/(m^2.s) air flow and 35 kW/m^2 heat flux. A peak PN concentration of $1x10^{10}$ /cc at a particle diameter for the peak number of particles at 20 nm was found [15]. Altaher et al. [17] reported a peak PN of $5x10^8$ /cc at 30 nm for the lean combustion of biomass pellets in a biomass heater. This shows higher particle number and a smaller size for gasification conditions, and this will be investigated for sweet sorghum in the present work, which will be the first investigation of gasification of sweet sorghum stalks. It is possible that the BGG when burnt in an engine or burner has its fine particulate content destroyed, but this was not investigated in the present work. The BGG gas fine PM content has the potential to foul the air intake system including the valves and so knowledge on this problem is essential for future practical use of BGG for clean energy generation as electricity or heat.

2. Methodology

The materials used for the gasification tests were sun-dried sweet sorghum stalk residue, grain sorghum stalk residue and corn stalk residue. The biomass composition analysers used were Mettler Toledo Thermogravimetric Analyser (TGA)/DSC3+, Thermo Scientific Elemental Analyser 2000, Parr 6200 bomb calorimeter. The gasification test rig is shown in Fig. 1 and consisted of the Cone calorimeter, Agitent Data logger, Gasmet FTIR gas analyser (CR2000), portable oxygen analyser, and Cambustion DMS500 particle size analyser. The operational method in gasification mode was as developed by Irshad [13] and used previously on pine cribs [2,15].

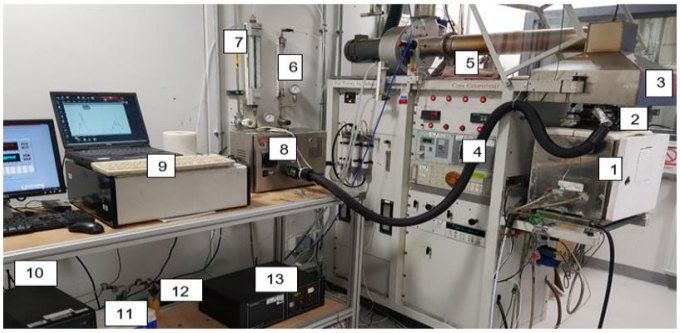

1. Restricted ventilation box
2. Chimney stack
3. Secondary air entrainment duct
4. Heated line
5. Sampling point for DMS500
6. Flow meter (nitrogen)
7. Flow meter (air)
8. FTIR pump
9. Gasmet FTIR
10. Computer (ConCalc5 programme)
11. Condenser
12. Silica gel
13. O_2 analyser

146

147 Fig. 1 The Cone calorimeter and the associated gas analysers

148 **2.1 Cone calorimeter small scale gasifier**

149 A modified controlled atmosphere cone calorimeter was used, with a sealed air box around
150 the burning biomass and the air supply controlled so that the metered equivalence ratio $Ø_m$
151 could be varied by varying the air flow. The original version of this cone calorimeter equipment
152 had considerable development before it was used in the present work [13].
153 Insulating fibre board lined the gasification chamber, the internal dimensions of the box were
154 0.33 m long, 0.275 m wide and 0.305 m high. A metered flow of air was supplied to the sealed
155 box from two openings in the bottom. A calibrated variable area flow meter was used to
156 determine the flow rate of air so that the metered equivalence ratio, $Ø_m$, of the gasification
157 could be controlled. The mode of gasification is usually referred to as fixed bed updraught
158 gasification. This is because the biomass to be gasified is solid in its raw form and has a fixed
159 location and is not agitated as in some gasifiers, such as fluidised bed gasifiers, which operate
160 at constant temperatures throughout the bed. The air flow goes upward from the bottom of the
161 test chamber over the test section and up the chimney, so it is an updraught gasifier.
162 Commercial gasification or log boilers are all fixed bed gasifiers in the primary stage but can
163 be either downdraught, or updraught as in the present experiments and several commercial
164 log gasification boilers [2].

165

2.2 Proximate analysis

The inner and outer core samples were obtained by separating them from the stalks of the biomass residues. Thereafter, size reduction of the whole stalks, inner and outer cores was done by cryo-milling.

The proximate analysis of the tested biomass samples was carried out using the Mettler Toledo TGA. Nitrogen gas was blown through the analyser at the beginning of the TGA at 50 ml/min. Towards the end of the TGA (in the last 15 minutes), air was blown through the analyser at 50 ml/min for the oxidation of Fixed Carbon (FC) and ash. The temperature profiles of the TGA analysis are presented graphically in Figs. A1 to A3. The CHNS-O (elemental) analysis of the biomass residues was carried out on the Thermo Scientific Elemental Analyser 2000, while fuel characterisation was carried out using the Parr 6200 bomb calorimeter. The carbon and oxygen balance method of Chan and Zhu [18] was utilised to calculate the stoichiometric AFR of the biomass from the elemental analysis. The test rig operational rich equivalence ratio (ϕ) was determined from the mass loss of the test sample and the metered air flow into the gasifier. This enabled the gasification AFR (metered AFR) by mass to be determined. The equivalence ratio of the gasifier was the ratio of the stoichiometric AFR (determined by carbon balance from the elemental analysis [18]) to the measured AFR (Equation 1). The metered AFR was determined from Equation 2.

$$\phi = \frac{stoichiometric\ AFR}{metered\ AFR} \quad (1)$$

$$metered\ AFR = \frac{metered\ air\ flow,\ \ g/s}{mean\ mass\ loss\ rate,\ \ g/s} \quad (2)$$

The speciation of the sampled raw gases was carried out using the Gasmet heated FTIR analyser. The concentration of hydrogen in the sampled gas was estimated from the equilibrium constant (K) for the water-gas shift reaction (Equations 3 and 4) [19].

$$CO + H_2O \rightleftharpoons CO_2 + H_2 \qquad \Delta H^o_{298} = -41.1\ \frac{kJ}{mol} \quad (3)$$

$$K = \frac{[CO_2][H_2]}{[CO][H_2O]} \quad (4)$$

$[CO_2]$, $[H_2]$, $[CO]$, and $[H_2O]$ in Equation 3 represent the concentrations of carbon dioxide, hydrogen, carbon monoxide, and water vapour, respectively. The value that was used for K in Equation 4 was 3.5, corresponding to an equilibrium temperature of 1,738 K [18].

2.3 Sample preparation

Fig. 2 (a) and (b) depicts the prepared sweet sorghum stalk residue samples in the sample holder as well as the transverse section of the stalk residue. The test samples were prepared by cutting the stalks and stacking them into a 100 x 100 mm sample as depicted in Fig. 2(a). The composite nature of the stalk residue is depicted in Fig. 2 (b).

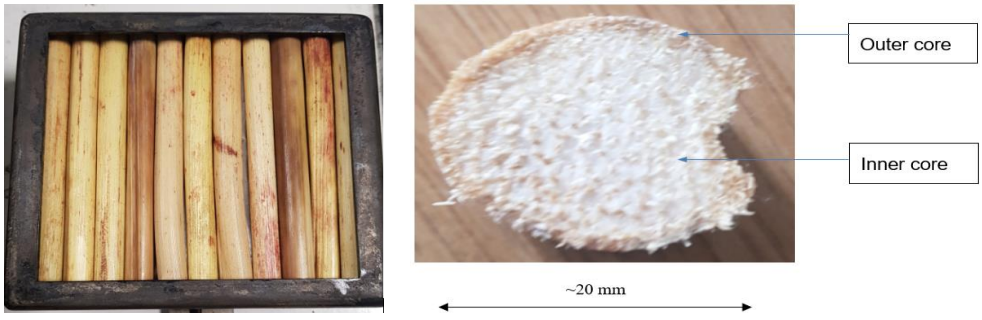

(a) (b)

Fig. 2 Preparation of sweet sorghum stalk residue for the gasification test: (a) Biomass sample in the sample holder (b) Transverse section of sweet sorghum stalk

2.4 Test conditions

Table 1 shows the air flow conditions for the gasification test. The radiant heat flux that was used during the test was 25 kW/m^2. This was lower than the 35 kW/m^2 advocated by Irshad [12, 13] for pine wood and this was because sweet sorghum released volatiles at a lower temperature than for pine wood, so the radiant heater in the cone calorimeter was reduced in power. This is equivalent to operating the gasifier at a lower temperature than for wood gasification.

Table 1 Biomass gasification test conditions

Air flow rate, lpm	Air flux, g/ (m^2.s)
4.4	9.0
5.5	11.2
6.3	12.9
7.0	14.3
7.6	15.5
8.0	16.3
9.4	19.2

2.5 Heat Release Rate (HHR)

The total or overall HRR (THRR) was determined from the cone calorimeter diluted gas sample analysis using oxygen consumption calorimetry [20]. The gasification gas emerging from the exit duct above the cone calorimeter was combusted with the entrained ambient air used in the cone calorimeter. The diluted sample was analysed for its oxygen content which was used to determine the overall HRR. FTIR analysis of this sample showed that combustion was complete and CO and hydrocarbons were very low. The THRR was also obtained by multiplying the mass loss rate (MLR) by the Higher Heating Value (HHV) of the biomass. There was good agreement in the two methods.

The primary HRR (PHRR) in the gasifier was determined by carbon balance from the dry oxygen analysis after the FTIR. The dry oxygen was converted to a wet oxygen using the water vapour measured by the FTIR, the oxygen balance method requires the oxygen to be on a wet basis for HRR analysis. The difference in the THRR and PHRR is the secondary HRR (SHRR) which is the maximum HRR in the application that the gas is used for: heat, gas turbine or diesel engines for power generation, which was the application of the present work.

2.6 Measurement of the Hot Gases Efficiency (HGE)

The Hot Gases Efficiency (HGE) for the gasification of the biomass was estimated from Equation 5.

$$HGE = \frac{(HHV\ of\ the\ product\ gases + sensible\ heat\ of\ the\ gases)\left(\frac{MJ}{kg\ biomass}\right)}{HHV\ of\ the\ biomass\ fuel\left(\frac{MJ}{kg\ biomass}\right)} \quad 5$$

The HHV for each of the product gases was obtained by multiplying the HHV of the gaseous component (MJ/kg species) by the Emission Index (EI) of the species (kg species/kg biomass). The reference temperature that was used Equation 5 was the room temperature (20 ^{o}C). All the measured species with an energy content had the EI determined and converted to heat release and then all the heat release values were added together to get the total hydrocarbon heat release.

3. Results and discussion

3.1 Biomass analytical test results

The outer and inner cores shown in Fig. 2b were analysed separately and their weight percentages are given in Table 2. This shows that the inner core, although having more volume has lower mass, indicating that the core has a low bulk density for all three biomasses. The CHNS-O, TGA, and bomb calorimetry test results for the three biomass residues are presented in Tables 3, 4, and 5 respectively. The gasification parameters (AFR and $\boldsymbol{\emptyset}$) presented in Table 6 for the tested conditions of air flow were estimated from Equations 1 and 2 and the stoichiometric AFR data (Table 5). Table 3 shows that the inner and outer cores have a similar composition, in spite of the difference in bulk density. All parts of the stems have a high oxygen content, much higher than for wood and this results in a low stoichiometric AFR, which means less air is required to achieve the gasification mixtures compared with wood. The moisture content, Volatile Matter (VM), Fixed Carbon (FC), and ash contents of the crop residues are given in Table 4 and are quite similar to the two layers, although there is

some evidence that the ash is concentrated in the inner layer, which indicates that wind blown dust ash is not significant as this would accumulate in the outer layers.

Fig. 3 shows the TGA results of the tested crop residues. Tables 3, 4, and Fig. 3 (the CHNS-O test and the TGA results) show that the physical properties of the inner and the outer cores of the tested biomass residues were quite different. Fig. 3 also shows that the moisture in the samples began to evaporate at temperatures below the boiling point of water (50 ^{o}C to 54 ^{o}C). Liquids are known to evaporate within a wide range of temperatures below their boiling points when the TGA samples are placed in open crucibles [21]. Fig. 3 shows that the volatile release had two phases: 70% of the mass released by heating between 200 and 350 ^{o}C and 15% of the mass released as high boiling point organic compounds between 350 and 880 ^{o}C. The first rapid release of flammable volatiles creates the rich mixtures that form the gasification mixture.

The nitrogen contents of the composite stalk residues were estimated by adding the products of the nitrogen contents of the components of the residue (inner and outer cores) and their corresponding weight fractions (Table 2). The Fuel Bound Nitrogen (FBN) content of SSS is high and if this was burnt in open fires would result in high NO emissions. However, in gasification FBN is converted to N_2 and thus the problem of high NO emissions is avoided.

The element per carbon ratio of sweet sorghum, grain sorghum and corn stalks were estimated from the CHNS-O test results and presented in Table A1.

Table 2 Weight percentages of inner and outer cores of the tested residues

Biomass	**Inner core, wt%**	**Outer core, wt%**
Sweet sorghum	30.00	70.00
Grain sorghum	25.00	75.00
Corn	21.88	78.13

274 Table 3 Biomass residues CHNS-O test results

Stalk	**Component**	**C, wt%**	**H, wt%**	**N, wt%**	**S, wt%**	**O, wt%**
Sweet sorghum	Whole	41.20	6.21	0.52	0	51.57
	Inner core	40.70	5.80	0.8	0	52.70
	Outer core	41.44	5.58	0.4	0	52.58
Grain sorghum	Whole	43.11	5.97	0.27	0	50.58
	Inner core	42.43	5.93	0.28	0	51.36
	Outer core	43.92	6.11	0.27	0	49.70
Corn	Whole	43.65	6.01	0.44	0	49.94
	Inner core	39.75	5.96	0.92	0	53.37
	Outer core	44.08	5.82	0.31	0	49.79

275

276 Table 4 Biomass residues TGA results

Stalk	**Component**	**H_2O, wt%**	**VM, wt%**	**FC, wt%**	**Ash, wt%**
Sweet sorghum	Whole	10.75	71.14	17.96	0.15
	Inner core	7.78	74.25	15.72	2.24
	Outer core	6.29	75.17	17.5	1.05
Grain sorghum	Whole	7.86	74.08	17.41	0.66
	Inner core	8.39	73.03	17.46	1.13
	Outer core	7.50	72.07	19.22	1.22
Corn	Whole	7.69	71.68	19.29	1.34
	Inner core	6.37	73.21	17.06	3.37
	Outer core	6.94	71.13	19.85	2.09

277

278

279

280 Table 5 Biomass stoichiometric AFR and Gross Calorific Values (GCV)

Biomass stalk residue	**Stoichiometric AFR**	**GCV, MJ/kg**
Sweet sorghum	4.57	17.97
Grain sorghum	4.79	17.37
Corn	4.89	17.51

281

282 Table 6 Estimated AFRs and equivalence ratios (Ø) for the gasification tests

Test conditions		**Estimated gasification parameters using Equations 1 and 2**	
Air flow rate, lpm	**Air flux, g/ (m^2.s)**	**AFR**	**Ø**
4.4	9.0	1.3	3.6
5.5	11.2	1.9	2.4
6.3	12.9	2.2	2.1
7.0	14.3	2.4	1.9
7.6	15.5	2.8	1.6
8.0	16.3	3.1	1.5
9.4	19.2	3.3	1.4

283

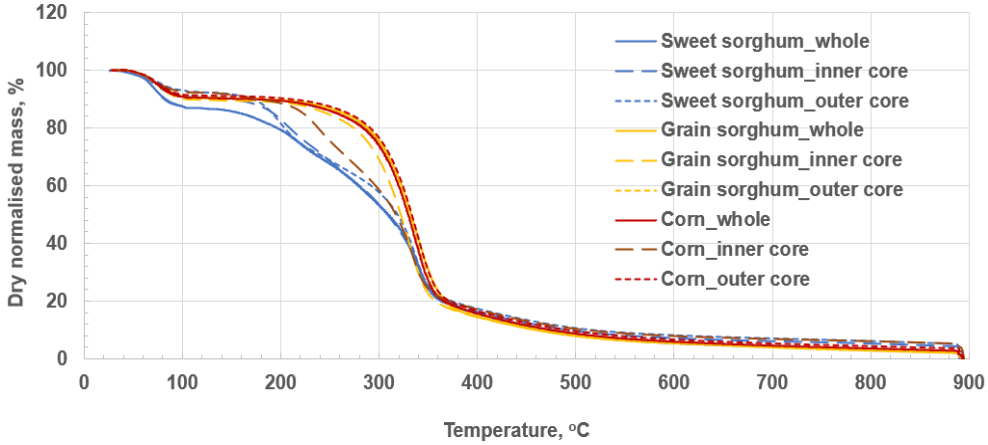

284

285 Fig. 3 TGA profiles for the tested biomass residues (whole stalks, inner and outer cores)

3.2 Mass Loss Rate (MLR) profiles for sweet sorghum stalk residues

The normalised mass loss and the Mass Loss Rate (MLR) profiles for the gasification of sweet sorghum stalk residues at the tested air flow conditions are shown in Figs. 4 and 5 respectively. Fig. 4 shows that at the end of the test when the flame had gone out there was a remaining mass that had not been gasified which varied between 30% of the initial biomass mass for 19.2 kg_{air}/m^2s to 15% at 11.2 kg_{air}/m^2s, which is similar to the fixed carbon of 18% in the TGA analysis. This was undergoing smoldering combustion as the mass was still reducing slowly in Fig. 4 and the mass loss rate in Fig. 5 goes to a low value at the end of the test, but not to zero. Smoldering combustion is a very slow char oxidation rate. It is shown in the energy analysis of the results that the hot gases efficiency (HGE) of the process is 81% at the optimum Ø, but lower for other biomass. It is likely that the inefficiency is due to the char produced not being efficiently gasified. Also, the energy in char per kg is 1.64 times the energy in the original biomass, thus if char is not gasified then this will limit the HGE.

Four stages (A, B, C and D) were identified during the rich burning of the sweet sorghum biomass residue, as shown in Fig. 6 for the 16.3 $g/(m^2.s)$ air ventilation condition. The period of negligible mass loss, during which the gradient of the normalised mass loss profile was zero, represents the Ignition Delay (ID) for the test (the duration between the test start time and the auto-ignition of the biomass sample). The ID of the sweet sorghum stalk samples for the tested conditions ranged from 7 s to 25 s. The auto-ignition of the sample was followed by a period of rapid loss in mass due to the rapid burning of the biomass sample in the air inside the compartment at the start of the test (stage A). Stage A was initial lean combustion using the air in the chamber at the start of the test as well as that supplied to the chamber. Stage A was followed by the steady state flaming gasification phase (B). This is the steady state gasification period of the test in terms of steady mass loss rate and relatively constant HRR as shown in Fig.7. Stage C is the char combustion stage (C) but with some visible flame, due to CO combustion, and a lower rate of mass loss than the flaming gasification phase B. The end of stage C was the flameout time (420 s for the 16.3 $g/(m^2.s)$ air flow condition. Stage

313 D was the smoldering combustion phase giving a mass loss but with no flaming combustion.
314 The flame photographs for different stages are shown in Fig. 6 (b), (c), and (d).

315 The AFR and the yield of the products of gasification were determined when the gasification
316 was at steady state. It is shown later that steady state gasification occurs later when CO and
317 THC are roughly constant and this period is about 120 – 220 s. The delay in the establishment
318 of steady state gasification conditions is the delay in heat transfer to the biomass sample,
319 which releases volatiles as the heat is conducted through the biomass fuel. This fuel heat-up
320 period was shown for pine wood by Irshad [13] using imbedded thermocouple, which were not
321 practical to attach to the sweet sorghum stalks.

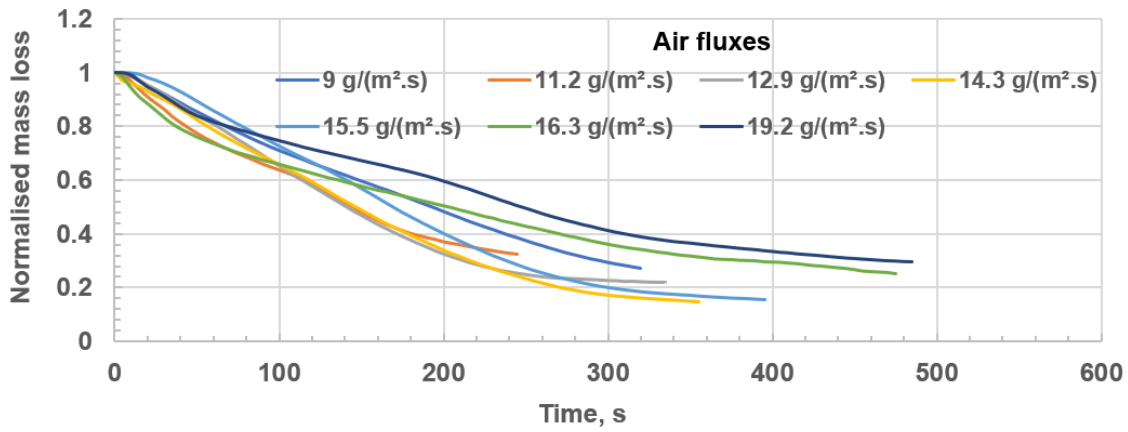

322

323 Fig. 4 Normalised mass loss profiles for the gasification of sweet sorghum stalk

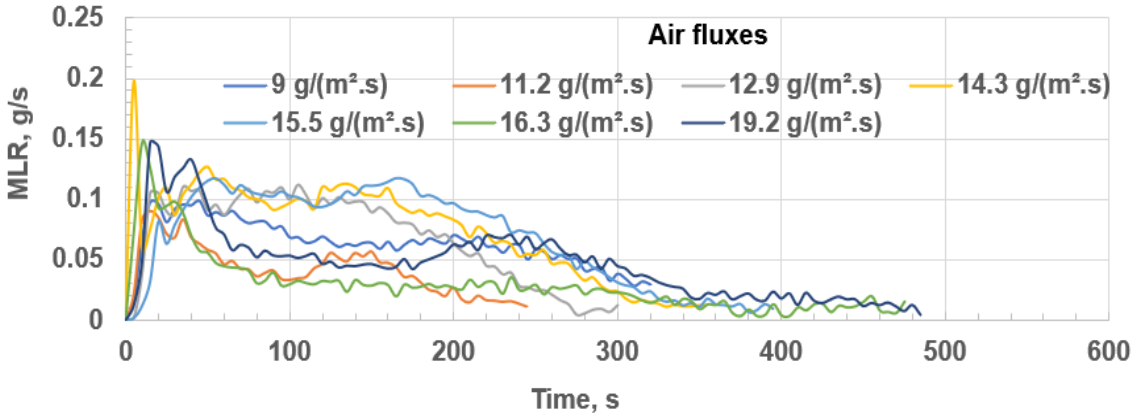

324

325 Fig. 5 Mass Loss Rate (MLR) profiles for the gasification of sweet sorghum stalks for different
326 air fluxes

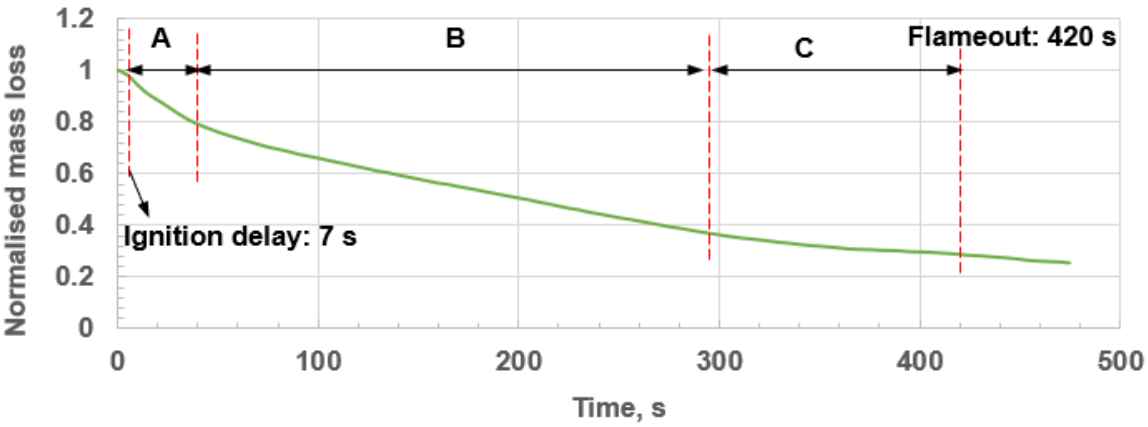

(a)

(b) (c) (d)

Fig. 6 Stages of the gasification: (a) Normalised mass loss profile of sweet sorghum stalk residue at 16.3 g/(m^2.s) air flow (b) Rapid combustion Phase A (c) Steady state gasification flame Phase B (d) char combustion Phase C

3.3 Equivalence ratios (Ø)

The measured AFRs and equivalence ratios (Ø) for each air flow are shown in Table 6, which shows that Ø decreased as the air flow was increased. This was because the rate of consumption of fuel in the gasifier is a linear function of the air flow as for all fuels the HRR is close to 3 MJ/kg_{air}. Thus, increasing the air flow increases the fuel consumption while the oxidation tends towards complete combustion. This makes the gasification zone leaner. Table 6 shows that increasing the air flow changed the equivalence ratio from 3.6 to 1.4, which is the range within which optimum gasification was observed to occur for the investigated biomass residues.

3.4 Heat Release Rate (HRR) profiles for sweet sorghum stalk residues

The primary and secondary HRR profiles (PHRR and SHRR) for the 9 g/(m^2.s) test condition for sweet sorghum stalk is shown in Fig. 7. The peak PHRR in Fig. 7 occurred immediately after auto-ignition with the initial volatile release burning in the air in the gasifier with a high HRR. Once the only air available was from the air inlet, the mixture became richer and combustion flames were replaced by gasification with low PHRR. Fig. 7 also shows the period of steady state total HRR (+/- 10%) for the 9 g/(m^2.s) condition was from 65 to 130 s. Gasification of the exposed top surface of the sample (the outer core) occurred immediately after the auto-ignition of the sample. The burning of the exposed top outer core exposed the inner core of the stalks to the flames. After 200 s, (Fig. 7) the inner core was burned up thereby exposing the outer core at the base of the sample holder. The gasification of the outer core at the base of the sample holder led to the third PHHR peak. Therefore, the period of steady state gasification of the composite biomass was carefully delineated as the period between the end of the gasification of the exposed (top) outer core and the beginning of the gasification of the outer core at the bottom (after 200 s for the condition shown in Fig. 7). In this manner, the true steady-state HRR period for the composite material (both outer and inner cores) was marked out so that the period of gasification of the outer core alone was not erroneously included in the delineation.

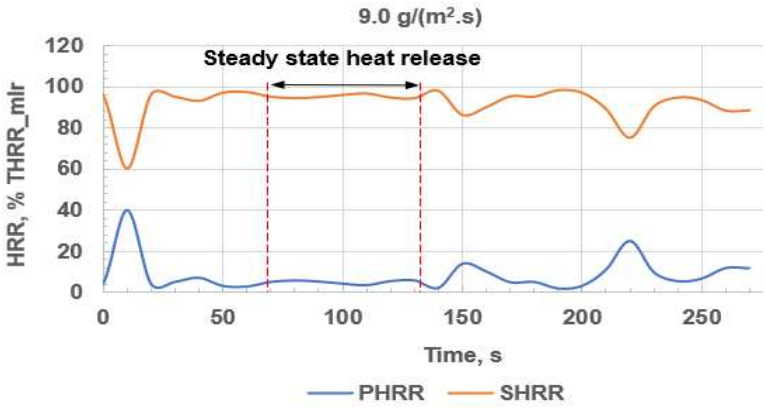

Fig. 7 PHRR and SHRR profiles for the 9 g/(m^2.s) test condition (Ø=3.6)

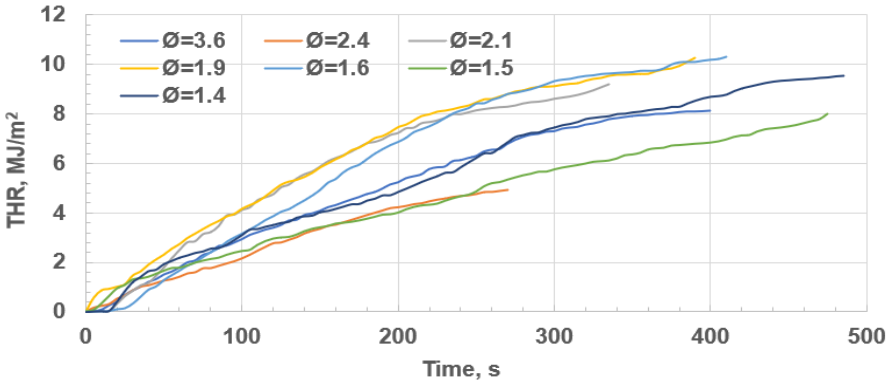

364

365 Fig. 8 Total Heat Release (THR) profiles of sweet sorghum stalks

366 The Total Heat Release (THR) profiles for all the tested conditions are shown in Fig. 8. The
367 duration of the test was different for each of the investigated conditions due to the non-uniform
368 diameter of the stalks. The diameter of the stalks ranged from 15-20 mm. The THR for the
369 gasification of the sweet sorghum stalks for equivalence ratios (Ø) between 1.6 and 2.1 were
370 relatively high compared to the THR at the other Ø values. This suggested that the optimum
371 Ø for the gasification of the sweet sorghum stalk would be between 1.6 and 2.1.

372 **3.5 Evolution of CO and THC during the rich burning of sweet sorghum stalks**

373 Figs. 9 and 10 show the evolution of CO and THC (total hydrocarbons) gases from the
374 gasification of the sweet sorghum stalk residues. The THC values were calculated from the
375 FTIR concentrations of the hydrocarbon compounds (Table A2) by converting the FTIR
376 concentrations of the hydrocarbons to their methane equivalents. The FTIR concentration of
377 each hydrocarbon compound was converted to the methane equivalent by multiplying the
378 measured concentration by the number of carbon atoms in the compound. Thereafter, the
379 methane equivalents of the species for each of the tested air flows/conditions were summed
380 up to obtain the THC for the air flow. The spikes in the concentration profiles that occurred
381 within the first 50 s of the gasification were as a result of the initial lean combustion at the start,
382 as the compartment with the gasification material inside was full of air at the start and it takes
383 time before gasification steady state is achieved. This initial lean combustion gave rapid

384 combustion of the test samples immediately after auto-ignition as shown in Fig. 6 (a) and (b)
385 and in the HRR results in Fig. 7.

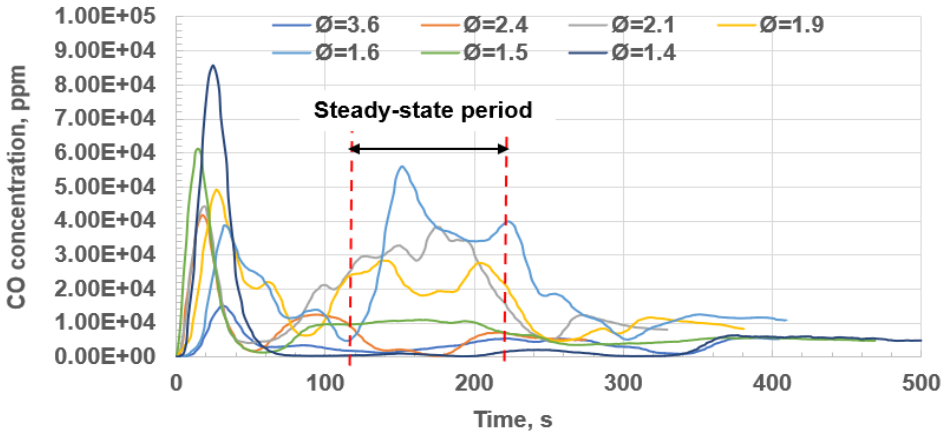

386

387 Fig. 9 Evolution of CO from the primary stage of the gasification

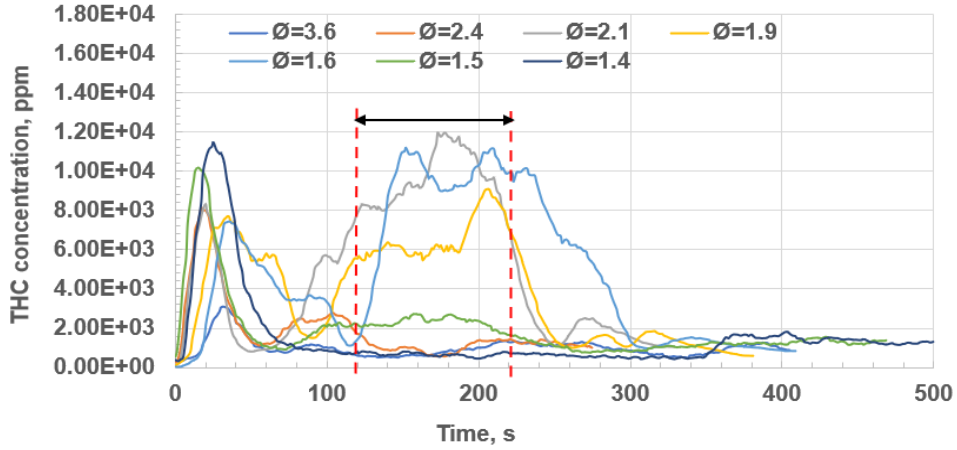

388

389 Fig. 10 Evolution of THC from the primary stage of the gasification

390 The effect of steady state gasification on the evolution of CO and THC gases is shown in Figs.
391 9 and 10, which show that the highest CO and THC were for Ø = 1.6 – 2.1, with lower values
392 for leaner and richer mixtures. This is the optimum gasification condition which yields the
393 highest energy content in the biomass gasification gas (BGG) in the period 120 s – 220 s after
394 the start of the test. This is the steady state gasification period and would be longer if more
395 mass of sample had been used. The results depicted in Figs. 9 and 10 show that the optimum
396 gasification condition with the maximum yield of CO and THC was for an air flux of 13 – 14

g/ms^2 with an equivalence ratio, Ø, of about 2. The objective of the gasifer was achieved with low heat release but good gasification and release of CO, hydrocarbons and hydrogen which burn in the second stage combustion after the outlet from the gasifier chimney when ambient air is entrained. During the gasification period oxygen was depleted in the flue, which will be the same as the oxygen in the gasifier, as shown in Fig. 11.

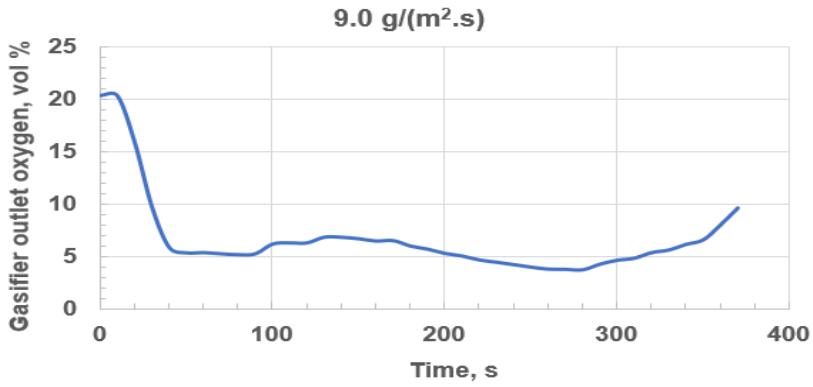

Fig. 11 Gasifier outlet oxygen as a function of time.

Phase C in Fig. 6a, after 300 s had low CO and THC at all air ventilation rates, yet there was a significant but low mass loss rate, as shown in Fig. 5. This is the char combustion phase after all the volatiles have been gasified. There was an observable flame in this period, as shown in Fig. 6d, which would be a CO flame. At the end of the char combustion Phase C, the flame was observed to go out, but smoldering combustion remained, as shown in Fig. 6d, as there was a continuing mass loss. There was a transition from gasification near-zero oxygen-rich combustion to char combustion after 350 s. The increase in oxygen in the char combustion region showed that the char was not being gasified but was burning in oxygen. This is the key reason for the inefficient conversion of biomass energy to BGG energy.

This change from biomass gasification to char oxidation had an influence on the gasifier exit temperature as shown in Fig. 12, for the optimum gasification at Ø=1.9. In the peak gasification phase from 120 to 220 s, deduced from the CO and THC results, Fig. 12 shows that the gasifier outlet temperature was constant at the average temperature of 380 ^{o}C or 657 K. This

418 is a much lower temperature than the 800 – 900 °C used in many gasifiers [22]. This is because
419 it is the hydrocarbon volatiles evolved from the biomass that is being gasified initially. After
420 220 s the mass burn rate decreases due to the start of char combustion in the surplus oxygen
421 that occurs due to the change of stoichiometric AFR for char compared to the biomass. To
422 gasify the char phase the temperature in Fig. 12 would be increased, as discussed above, by
423 reducing the air flow to produce rich char gasification conditions with near-zero oxygen. This
424 could be achieved in a practical application of batch gasification with the increase in oxygen
425 signaling a requirement to reduce the air flow until the temperature increased and oxygen was
426 near-zero.

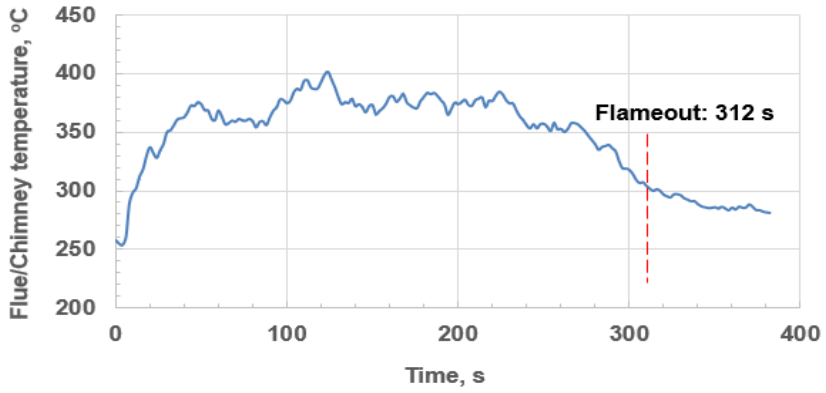

427

428 Fig. 12 Flue (chimney) temperature profile for the gasification of sweet sorghum stalk residue
429 at Ø=1.9

430 The slower rate of burning for char gave rise to an increased oxygen level as the gasification
431 conditions for char are quite different from those for the raw biomass. The oxygen
432 concentration increased with char combustion due to operation at constant air flow. If char is
433 assumed to be pure carbon then the stoichiometric AFR is 11.5/1 which is much higher than
434 for the sweet sorghum biomass which was 4.6. For a constant air flow this means that the char
435 mass burn rate would be lower than for the biomass by a factor of 2.5, but the HRR would be
436 similar as the GCV for Char is 29.6 MJ/kg compared with 18.0 for sweet sorghum. The heat
437 release per kg of air for char is 2.57 MJ/kg_{air} and 4.0 MJ/kg_{air} for sweet sorghum, so if the air
438 flow is constant to the gasifier then char mass burn rate will be 63% lower than for sweet

sorghum for the same heat release in MJ, as shown in Fig. 5 for the char burning Phase C. However, the mass burn rate in the char phase is much lower than 63% of that in the biomass gasification phase and this is because the optimum gasification temperature for char is higher than for biomass at about 1,200 K. The effect of this is to make the gasification conditions for char leaner and thus less optimum for the generation of CO and hydrogen. This is why the CO is lower in Fig. 9 in the char burning phase. For the gasifier to convert char to CO it needs to operate richer with reduced air flow, also water injection helps the conversion of carbon to hydrogen, as well as CO to hydrogen and CO_2. For batch gasification of biomass, future work will investigate reducing the air flow in the char gasification stage and increasing the hydrogen yield with water injection into the residual char.

3.6 Estimation of the optimum Ø for the gasification of sweet sorghum stalk residue

The yields of the combustible gases (CO, H_2, and THC) that were evolved during the gasification of the crop residues were averaged at steady state for the air fluxes that were tested. The THC yield was computed in terms of the methane (CH_4) equivalent of the emitted hydrocarbon gases. The estimated yields (in g/kg biomass residue) as well as the flow rates of the combustible gases were plotted against the equivalence ratios as shown in Figs. 13 and 14 respectively.

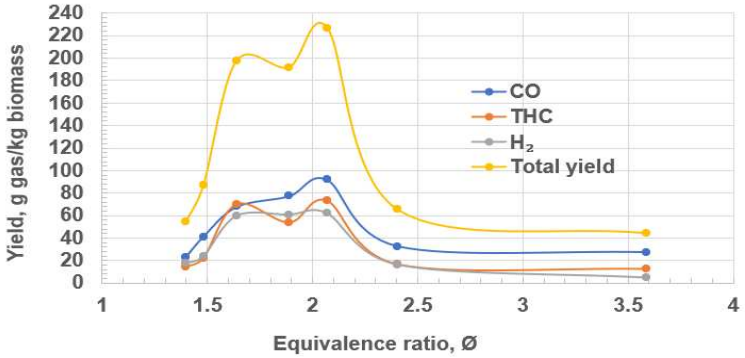

Fig. 13 Yield of combustible gases from the gasification of sweet sorghum stalk residue

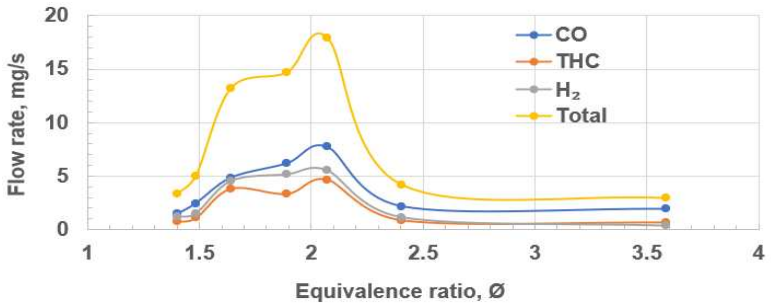

Fig. 14 Flow rate of combustible gases from the gasification of sweet sorghum stalk residue

Fig. 13 and 14 show that the maximum yield and flow rate of the combustible gases occurred at Ø=2.05 (≈2.1). The total hydrocarbons were an important part of the gas composition and energy transfer. It is important to keep the outlet gases hot in the transfer pipes to an engine or burner, so as to avoid condensation of the hydrocarbons and formation of tars. Many more traditional gasification systems have a poor HGE due to the loss of the tars, they see the tars as a problem not as an important part of the energy transfer from the biomass. The estimated optimum value of Ø (2.1) for the gasification of sweet sorghum stalk residue compared well to the value that was estimated for pine wood (2.8) by Irshad [2, 12, 13] using the same equipment. The optimum gasification Ø for sweet sorghum also compared well to the experimentally determined values for the stalks of grain sorghum and corn (1.7 and 1.9 respectively).

The Calorific Value (Cv), average molecular weight, and viscosity of the BGG at the optimum Ø for sweet sorghum stalk were 6.2 MJ/kg, 19.8 kg/kgmol, and 2.32 x 10^{-5} Pa.s respectively. The composition of the BGG at steady state biomass gasification for the three biomass residues investigated is given in Table 7 and these are comparable to those in the literature for biomass gasifiers [2].

480 Table 7 Biomass Gasification Gas (BGG) composition at steady state and optimum Ø (2.1)

BGG composition	Sweet sorghum	Grain sorghum	Corn	Pine wood
CO, %	3	0.8	1.2	14
H_2, %	28	19	16.8	8
CO_2, %	10	13.5	1.9	12
CH_4 (THC), %	4	0.7	0.8	8
H_2O, %	22	17.3	7.4	23
N_2, %	29	41	66	35
O_2, %	4	7.7	6	-

481

482 **3.6.1 Investigation of the relationship between the Maximum Flue Temperature (MFT),**
483 **Char Gasification Flue Temperature (CGFT), and equivalence ratio**

484 The maximum temperature of the flue/chimney (MFT) and the steady state Char Gasification
485 Flue Temperature (CGFT) for the tested air flows were determined from the gasifier outlet
486 chimney temperature profiles. The temperature profile of the chimney for the gasification of
487 the sweet sorghum stalk residue for the 14.3 g/(m^2.s) air flow condition is shown in Fig. 12.
488 The MFT for the condition (401 °C) occurred 124 s after the start of the test while the flameout
489 time was 312 s. The steady state temperature of the flue during char gasification (CGFT) was
490 about 380 °C. The MFT and the steady state CGFT values were plotted against the
491 equivalence ratios as shown in Figs. 15 and 16 for the stalk residues of sweet sorghum, grain
492 sorghum, and corn.

493

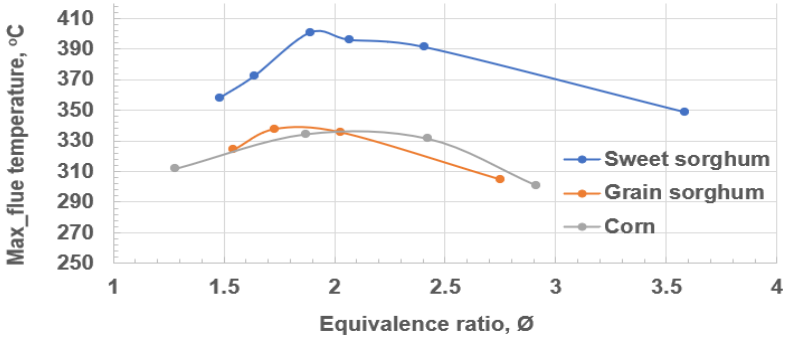

494

495 Fig. 15 Relationship between the Maximum Flue Temperature and equivalence ratio (Ø)

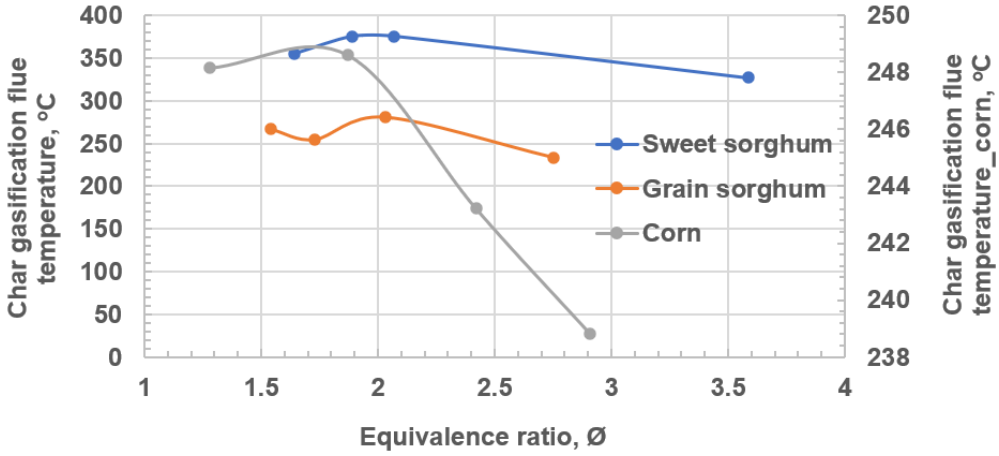

496

497 Fig. 16 Relationship between the Char Gasification Flue Temperature (CGFT) and
498 equivalence ratio.

499 Figs. 15 and 16, and Table 8 show that the MFT and the maximum steady state CGFT for the
500 crop residues occurred at Ø values that were approximately equal to the estimated optimum
501 equivalence ratios for the tested crop wastes in Table 6. Therefore, the optimum equivalence
502 ratio can be achieved in the biomass gasifier (designed for automatic operation) through
503 temperature control by adjusting the air flow to achieve the MFT for the biomass (Fig. 16).

504

505

506

Table 8 Relationship between the Maximum Flue Temperature (MFT), Char Gasification Flue Temperature (CGFT), and equivalence ratio

Biomass stalk	MFT, °C	CGFT, °C	Optimum Ø	Ø at peak temperature	
				MFT	CGFT
Sweet sorghum	401	375	2.1	1.9	1.9
Grain sorghum	340	280	1.7	1.7	2
Corn	337	249	1.9	2.2	1.8

3.6.2 Hot Gases Efficiency (HGE)

The Hot Gases Efficiency (HGE) of the investigated sweet sorghum stalk samples was estimated at the tested conditions from Equation 5. The HGE values were also estimated for the stalk residues of grain sorghum and corn. Fig. 17 compares the estimated HGEs to the HGE for pine wood. The estimated (maximum) HGE for sweet sorghum stalk residue in this work was 81% while the maximum HGE for grain sorghum and corn stalk residues were 52% and 46% respectively. The estimated HGE of 81% for sweet sorghum stalk residue falls within the top end of the range in the literature [2]. To improve these efficiencies the gasification of the residual char would have to be achieved.

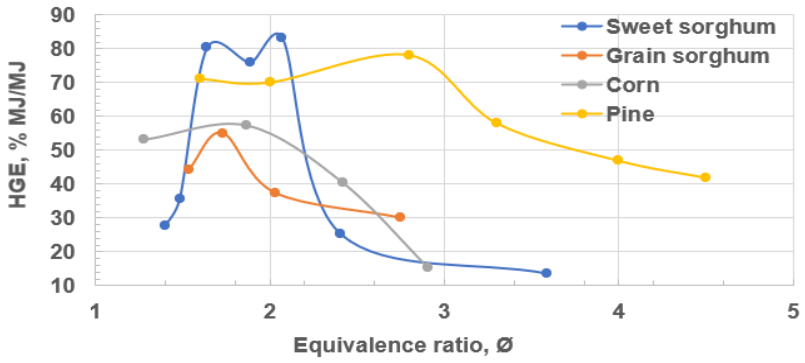

Fig. 17 Comparison of Hot Gases Efficiencies (HGE) of sweet sorghum stalk residue to other biomass

3.7 Particulate emissions from the gasification of sweet sorghum stalk residue

The Particulate Matter (PM) distributions for the gasification of sweet sorghum stalk residue at the tested conditions were estimated from the measured Particle Number (PN) distributions. The PM distributions were estimated at steady state after the measured data were corrected for dilution. The particles were assumed to be spherical with a particle density equal to that of carbon at 1,000 kg/m^3 (a common assumption in particle number to mass conversions).

3.7.1 Particle Number (PN) and Particulate Matter (PM) distributions for the gasification of sweet sorghum stalk residue

The Particle Number (PN) and Particulate Matter (PM) distributions for the tested conditions are given in Fig. 18 (a) and (b). Fig. 18 (a) shows that the tested conditions had PN peaks in the nanoparticles range (Dp < 30 nm). Generally, the observed peak PN concentrations (number of particles per cubic centimeter) in this work for the gasification of the stalk residue of sweet sorghum were much lower than the concentration that was reported for pine wood by Mustafa et al. [15] (1x10^{10} /cc). However, the peak PN concentration that was reported by Altaher et al. [17] (5x10^8 /cc at 30 nm) for the combustion of biomass pellet falls within the range of the peak PN concentrations for the gasification of sweet sorghum stalk residue (7.2x10^6 - 7.8x10^8 /cc).

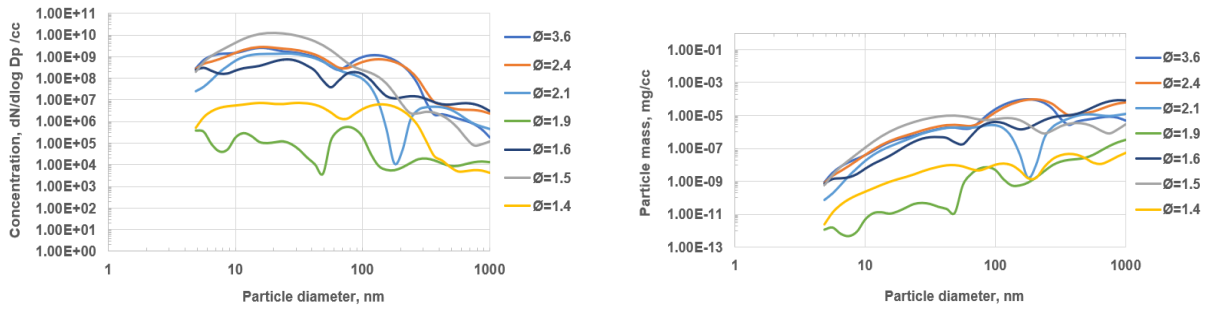

(a) (b)

Fig. 18 Comparison of PN and PM emissions for the tested air flows: (a) PN emissions for the tested air flows (b) PM emissions for the tested air flows

Mustafa et al. [15] reported for pine wood gasification an accumulation mode peak at 200 nm Dp which compared well to the observed accumulation mode Dp for the gasification of sweet sorghum stalk residue at 9, 11.2, and 19.2 g/(m^2.s) air flux conditions. Mustafa et al. [15] used the same method (Cone calorimeter) that was used in the current work in their investigation. Gaegauf et al. [23] reported that particles with Dp > 300 nm do not contribute substantially to total PN emission rate. The authors' report is in agreement with the PN results in the current work as Fig. 18 shows that the prominent PN peaks of the investigated modes occurred when Dp was < 300 nm. Fig. 18 shows that the peak PN resulted mostly from nanoparticles with Dp < 30 nm while the peak PM resulted from the fine particles. The fine particles are particles with Dp between 100 nm and 2.5 μm [24]. This 30 nm particle size range is that of the greatest health hazard on fine particles in the atmosphere and so this could be a source of combustion-derived nanoparticles, if the diesel engine or burner did not destroy the particles by combustion in oxidation reactions in the flames in the engine.

3.7.2 Particulate yield

The values for the particulate yield (in g particles/kg biomass) at the tested conditions for the gasification of sweet sorghum stalk were estimated from the measured PN distributions. Fig. 19 shows that the yield of particulates was lowest at the estimated optimum equivalence ratio (2.1).

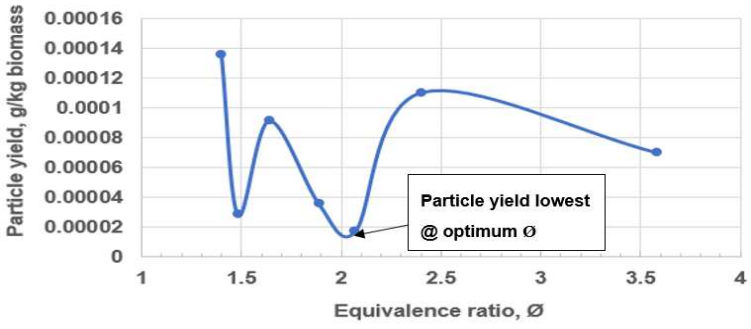

Fig. 19 Particulate yield as a function of equivalence ratio for the gasification sweet sorghum stalk residue

565 Johansson et al. [16] reported PM emissions of 62 to 180 mg/m^3 for pellet burners. However,
566 in the current work, the range of PM emissions for the gasification of sweet sorghum stalk
567 residue for the tested conditions was 104 to 730 mg/m^3. The observed disparity in the PM
568 results in the current work and the result in literature can be attributed to the peculiar composite
569 nature of the sweet sorghum stalks. Also, the sweet sorghum stalks were not pelletised prior
570 to the gasification test. The reported particle emission in ventilation-controlled compartment
571 fires for wood fires by Andrews et al. [25] (100 mg/m^3) compared well to the particle emission
572 of 104 mg/m^3 for the 12.9 g/(m^2.s) air flow condition in this work (the optimum condition). This
573 comparison is a little unfair to the gasifier gases as in a burner application air would be added
574 and a downstream flame achieved that would burn most of the particles from the gasification
575 stage. Similarly for diesel engine applications the engine would consume the particles as apart
576 from ash the particles will all burn.

577 **3.8 Explosive risk of syngas-air mixtures**

578 Two parameters that are commonly used to characterise the explosive behaviour of syngas-
579 air mixtures are the maximum explosion pressure and the maximum rate of pressure rise. The
580 results presented by Xie et al. [26] on the explosion behaviour of syngas (CO/H_2 50:50)-air
581 mixture show that stoichiometric and near-stoichiometric mixtures have relatively high
582 maximum explosion pressures (the explosion pressure peaked within equivalence ratio values
583 between 1 and 1.2). Also, when diluent gases (CO_2 and H_2O) were added to the initial CO/H_2
584 50:50 syngas, the maximum pressure decreased (the explosion pressure decreased as the
585 concentration of the diluent gases increased). The maximum rate of pressure rise was
586 reported to increase as the equivalence ratio increased. The authors reported the opposite
587 trend for the maximum rate of pressure rise when the concentrations of the diluent gases were
588 increased.

589 Table 6 shows that the equivalence ratios of the gas mixtures for the tested conditions were
590 > 1.2. The gasification products in Table 7 also contain diluent gases (CO_2 and H_2O).
591 Therefore, considering the results about the explosive behaviour of syngas in literature, it can

592 be inferred that during storage or usage in CI engines, the explosive risk of the gas in Table 7
593 with relatively high oxygen content will be low.

594 4. Conclusion

595 The Heat Release Rate (HRR) and particulate emission during the gasification of sweet
596 sorghum stalk were investigated in the current work by the restricted ventilation Cone
597 calorimeter method. The optimum gasification conditions for sweet sorghum stalk residue
598 were also determined.

599 The optimum air flux, equivalence ratio, Ø and HGE for the gasification of sweet sorghum stalk
600 residue were 12.9 g/m^2.s, 2.1 and 81% respectively. The optimum Ø and HGE values for the
601 investigated biomass residue (sweet sorghum stalk) compared well to the estimated value of
602 2.8 and 78% for pine wood. The Maximum Flue Temperature (MFT) and the maximum steady
603 state Char Gasification Flue Temperature (CGFT) for the tested crop residues occurred at Ø
604 values that were approximately equal to the estimated optimum equivalence ratios for the
605 residues. At constant air flow, the rate of combustion of the char that resulted from the
606 gasification of the biomass was slower than the rate of gasification of the original biomass
607 residue. This led to relatively lean combustion and low generation of CO during the char
608 combustion phase. The efficiency of char gasification in fixed bed biomass gasifiers can be
609 improved by reducing the flow rate of air to achieve rich burning conditions for char.

610 The results of the investigation showed that the peak PN emissions for the gasification of
611 sweet sorghum stalk residue occurred in the nanoparticles diameter range (Dp < 30 nm) at
612 the tested conditions. However, the yield of the particles was lowest at the optimum Ø
613 condition. Particles with Dp > 300 nm did not contribute significantly to the PN emissions from
614 the gasification of sweet sorghum stalk residue.

615 Acknowledgements

616 This work was supported by the Petroleum Technology Development Fund (PTDF), Nigeria,
617 the National Agency for Science and Engineering Infrastructure (NASENI), Nigeria, and the

Royal Society for an award “Investigating impact of E10 gasoline and its compositions on real driving emissions from in-service gasoline and hybrid vehicles, The IEC\NSFC\191747 – International Exchanges 2019 Cost Share (NSFC)”.

Appendix

Table A1. Element per carbon ratio of sweet sorghum, grain sorghum and corn stalks

Biomass	x (mols of C)	y (mols of H)	z (mols of O)	m (mols of N)
Sweet sorghum stalk	1	1.788	0.947	0.021
Grain sorghum stalk	1	1.647	0.881	0.007
Corn stalk	1	1.637	0.859	0.008

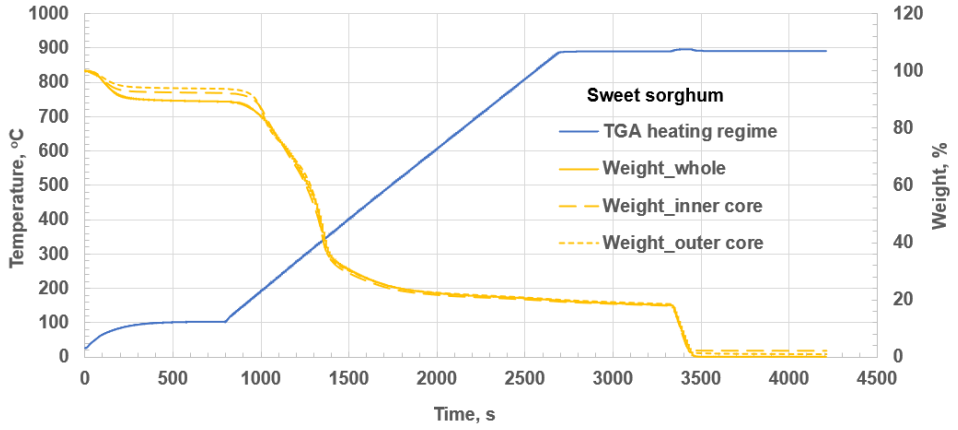

Fig. A1. Temperature and percentage weight versus time TGA profiles (sweet sorghum stalk residue)

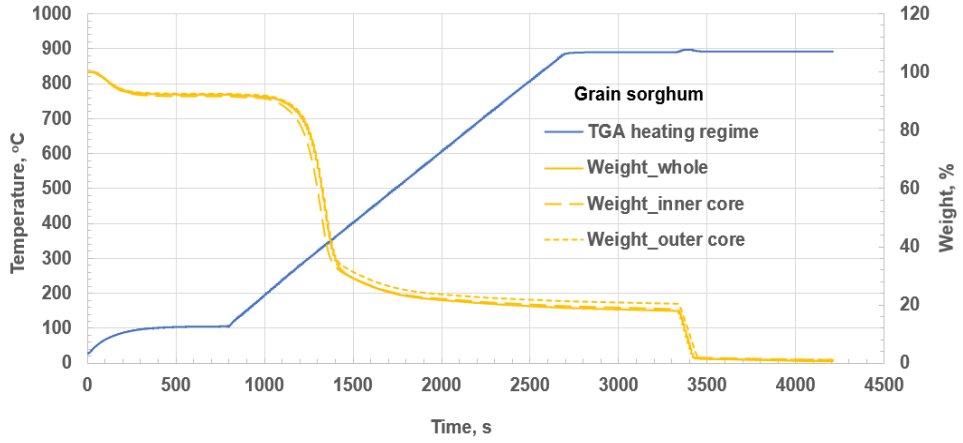

Fig. A2. Temperature and percentage weight versus time TGA profiles (grain sorghum stalk residue)

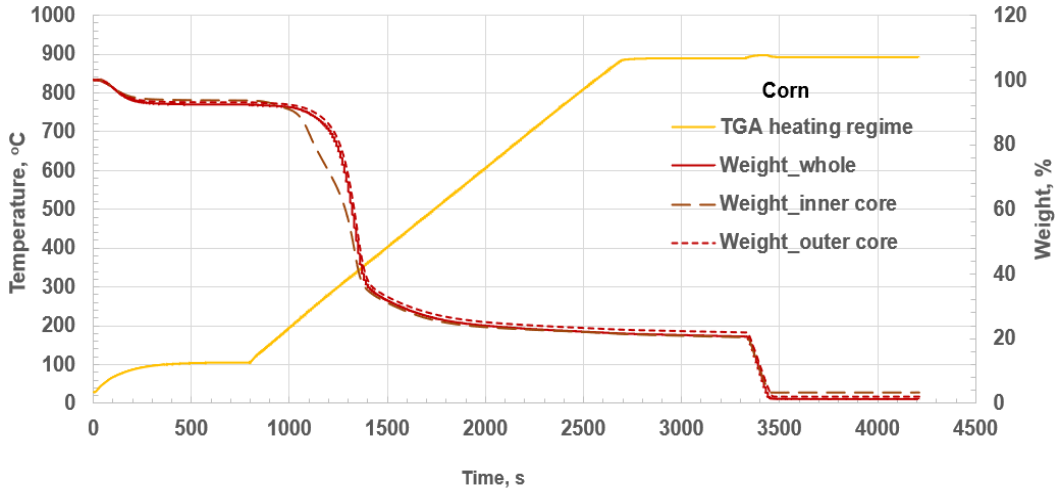

632

633 Fig. A3. Temperature and percentage weight versus time TGA profiles (corn sorghum stalk
634 residue)

635 Table A2. FTIR concentrations of hydrocarbon gases and selected organic compounds (ppm)

	Air flow, lpm	Methane	Hexane	Acetylene	Ethylene	Propene	Butadiene	Benzene	Toluene	O xylene	P xylene	1,2,3-TMB	1,2,4-TMB	Naphthalene	1-ethyl naphthalene	Formaldehyde	Acetaldehyde	Acetic acid	Acrolein
Sweet sorghum	4.4	495.9	26.9	752.7	410.9	138.9	17.3	125.8	22.8	61.2	64.7	94.8	240	31.8	57.2	70.5	24.4	28.1	85.4
	5.5	663.9	43.8	72.8	292.1	69.3	40.9	129.2	4.8	37.5	126.7	75.3	379.3	29.4	44.4	385.5	111.9	66.5	155.3
	6.3	2038.8	6.8	1008.6	1372.5	135.3	133	696	52	351	556	765	842	200	317	611	81	151	10
	7	1454.6	4.1	723	1102	126	100	491	35	130	511	414	695	117	176	541	64	105	10
	7.6	2310	7.4	637	988	90	83	583	115.8	319	303	637	707	173	275	386.7	41	84.7	22
	8	386.2	44.7	80.7	255.2	38.8	28.7	76.6	16.5	57.4	127.3	56.7	394.4	24.9	37.7	530	107.7	161	100.8
	9.4	325.1	62.4	47.3	114.3	99.6	26.1	66.5	22.1	19	81.5	36.4	225.2	10.8	16.4	147	32	36	99.5
Grain sorghum	4	416.5	17.4	48.6	338.8	69	16.5	29	43	27	371	42.5	495	3.9	14.7	773	125.7	255	44.4
	5.5	629.2	22.6	13.9	189	19	21.6	48.5	45.6	31.8	74.6	76.7	222	14	22.5	276.8	19.6	20.4	23
	7	357	25.6	16.2	188.5	38	25.6	28.5	38	31.5	89	35	335.6	10	13.6	383.7	57.3	63.7	31
	7.6	607	14.7	14.4	162	23.6	20.8	51	48.3	31.7	60.7	65	153	13.2	21	262	22.5	23	20.4
Corn	4	400.2	53	21	143	317.5	32.2	18.7	13	18.6	109	14	263	7	12.4	342	53	78	40
	5.5	333	76.8	23	226	67.8	21.2	34.5	16.1	54.5	149	39.7	335.4	10.8	17.8	455	73.4	158.9	46
	7	418	19.3	34	230	50.2	2	46	15	70.5	164.4	98.7	268.5	11.8	8	618.3	113.2	177	37.3
	7.6	424.6	30.1	19	157	27.8	17.7	34.2	37	11.4	76.5	33.7	241.6	9	15.5	338.3	30.7	36.8	22

636

References

[1] Simonyan KJ, Fasina O. Biomass resources and bioenergy potentials in Nigeria. African Journal of Agricultural Research 2013; 12(3):4975-4989.

[2] Andrews GE, Irshad A, Phylaktou, HN**,** Gibbs BM**.** Solid Biomass to Medium CV Gas Conversion with Rich Combustion. Proceedings of ASME Turbo Expo 2019: Turbomachinery Technical Conference and Exposition GT2019. ASME Technical Paper GT2019-90196. Phoenix, Arizona, USA; 2019.

[3] Song H, Yang G, Xue P, Li Y,Zou J, Wang S, Yang H, Chen H. Recent development of biomass gasification for hydrogen rich gas production. Applications in Energy and Combustion Science 2022; 10:100059. https://doi.org/10.1016/j.jaecs.2022.100059

[4] Alnouss A, McKay G, Al-Ansari T. Enhancing waste to hydrogen production through biomass feedstock blending: A techno-economic-environmental evaluation. Applied Energy 2020; 266: 114885. https://doi.org/10.1016/j.apenergy.2020.114885.

[5] Chianese S, Fail S, Binder M, Rauch R, Hofbauer H, Molino A, Blasi A, Musmarra D. Experimental investigations of hydrogen production from CO catalytic conversion of tar rich syngas by biomass gasification. Catalysis Today 2016; 277:182-191. http://dx.doi.org/10.1016/j.cattod.2016.04.005.

[6] Al-Zareer M, Dincer I, Rosen MA. Effects of various gasification parameters and operating conditions on syngas and hydrogen production. Chemical Engineering Research and Design 2016; 115:1-18. http://dx.doi.org/10.1016/j.cherd.2016.09.009.

[7] Mahishi MR, Sadrameli MS, Vijayaraghavan S, Goswami DY. A novel approach to enhance the hydrogen yield of biomass gasification using CO2 sorbent. Eng. Gas Turbines Power 2008; 130(1): 011501. https://doi.org/10.1115/1.2747252.

[8] Rith M, Buenconsejo B, Gitano-Briggs H, Biona JBM. Design and fabrication of a low-cost research facility for the study of combustion characteristics of a dual producer gas-diesel engine. J Engineering and Applied Science Research 2020; 47:447-57. https//doi.org/10.14456/easr.2020.48.

[9] Kousheshi N, Yari M, Paykani A, Saberi Mehr A, de la Fuente G. Effect of syngas composition on the combustion and emissions characteristics of a syngas/diesel RCCI engine. J Energies 2020; 13: 212. https//doi.org/10.3390/en13010212.5].

[10] Mahgoub BKM, Hassan S, Sulaiman SA, Mamat R, Abdullah AA, Hagos FY. Combustion and performance of syngas dual fueling in a CI engine with blended biodiesel as pilot fuel. J BioResources 2017; 12(3):5617-31.

[11] Guo H, Neill WS, Liko B. The combustion and emissions performance of a syngas-diesel dual fuel compression ignition engine. ASME paper no. ICEF2016-9367. 2016. https://doi.org/10.1115/ICEF2016-9367.

[12[Olanrewaju FO, Li H, Aslam Z, Hammerton J, Lovett JC. Analysis of the effect of syngas substitution of diesel on the heat release rate and combustion behaviour of diesel-syngas dual fuel engine. Fuel 2022; 312:122842. https://doi.org/j.fuel.2021.122842.

[13] Irshad A, Alarifi AA, Thompson S, Melton GJ, Andrews GE, Phylaktou HN, Gibbs BM. Use of the Cone Calorimeter for Investigating Biomass Gasification Staged Combustion. 22nd European Biomass Conference and Exhibition. Paper 2AO.4.1. Hamburg, Germany. 2014. p.388–98.

[14] Irshad A, Andrews GE, Phylaktou HN, Gibbs BM. Development of the Controlled Atmosphere Cone Calorimeter to Simulate Compartment Fires. In: Snegirev A, Liu NA, Tamanini F, Bradley D, Molkov V, Chaumeix N, editors. 9th International Seminar on Fire and Explosion Hazards (ISFEH9), Saint-Petersburg Polytechnic University Press; 2019. p.930-39. https://doi.org/10.18720/spbpu/2/k19-90.

[15] Mustafa BG, Kiah MHM, Irshad A, Andrews GE, Phylaktou HN, Li H, Gibbs BM. Rich biomass combustion: Gaseous and particle number emissions. Fuel 2019; 248:221-231. https://doi.org/10.1016/j.fuel.2019.03.027

[16] Johansson LS, Leckner B, Gustavsson L, Cooper D, Tullin C, Potter A. Emission characteristics of modern and old-type residential boilers fired with wood logs and wood pellets. Atmospheric Environment 2004; 38(25):4183-4195. https://doi.org/10.1016/j.atmosenv.2004.04.020.

[17] Altaher MA, Andrews GE, Gibbs BM, Hadavi SA, Li H, Jones E, et al. Comparison of Gaseous and Particulate Emissions from Wood Pellet and Oil Fired Combustion for the same Heat Input. 10th European Conference on Industrial Furnaces and Boiler (INFUB-10), Porto, Portugal. 2015.

[18] Chan SH, Zhu J. Exhaust Emission Based Air-Fuel Ratio Model (I): Literature Reviews and Modelling. SAE International paper no. 961020; 1996. https://doi.org/10.4271/961020.

[19] Choi Y, Stenger HG. Water gas shift reaction kinetics and reactor modeling for fuel cell grade hydrogen. Journal of Power Sources 2003; 124(2):432-439. https://doi.org/10.1016/S0378-7753(03)00614-1.

[20] Parker WJ. Calculations of the heat release rate by oxygen consumption for various applications. Department of Commerce, National Bureau of Standards, Centre for Fire Research: Washington, DC. 1982.

[21] Widmann G. Interpreting TGA curves. https://www.mt.com. 2001 [accessed 15 January 2021].

[22] Ngo SI, Nguyen TDB, Lim Y, Song B, Lee U, Choi Y, Song J. Performance evaluation for dual circulating fluidized-bed steam gasifier of biomass using quasi-equilibrium three-stage gasification model. Applied Energy 2011; 88: 5208-220.

[23] Gaegauf C, Wieser U, Macquat Y. 2001. Field investigation of nanoparticle emissions from various biomass combustion systems [Online]. 5th Conference on nanoparticle-measurement, Zurich. 2001.

[24] Kittelson DB. Engines and nanoparticles: a review. Journal of Aerosol Science 1998; 29(5):575-588. https://doi.org/10.1016/S0021-8502(97)10037-4.

[25] Andrews G, Ledger J, Phylaktou R. The gravimetric determination of soot yields in enclosed pool fires. 3rd International Seminar on Fire and Explosion Hazards. 2001. p.121-36.

[26] Xie Y, Wang X, Wang J, Huang Z. Explosion behaviour predictions of syngas/air mixtures with dilutions at elevated pressures: explosion and intrinsic flame instability parameters. Fuel 2019; 255:115724. https://doi.org/10.1016/j.fuel.2019.115724.